Magnetic domain patterns in Co_2MnGe Heusler nanostripes

K. Gross, P. Szary, O. Petracic, F. Brüssing, K. Westerholt, and H. Zabel
Institut für Experimentalphysik /Festkörperphysik, Ruhr-Universität Bochum, D-44780 Bochum, Germany
(Received 2 March 2011; revised manuscript received 20 June 2011; published 15 August 2011)

We have prepared thin films of the ferromagnetic Heusler alloy Co_2MnGe on *a*-plane Al_2O_3 substrates exhibiting growth-induced, superimposed fourfold and uniaxial magnetic anisotropies, the symmetry being determined by the single-crystalline Al_2O_3 substrate. The magnitude of the uniaxial anisotropy compared to the cubic anisotropy can be tuned over a wide range by the film thickness and the growth conditions. On submicrometer-wide stripes of Co_2MnGe prepared by electron beam lithography we studied magnetic domain patterns by magnetic force microscopy. For stripes with a sufficiently large uniaxial anisotropy and with the easy axis oriented perpendicular to the stripe axis, we find perfectly regular domain patterns with the magnetization direction perpendicular to the stripe axis and alternating from domain to domain. The highly regular and controllable domain patterns in Co_2MnGe nanostripes could be useful for magnetic storage devices and applications related to spin transfer torque.

DOI: 10.1103/PhysRevB.84.054456 PACS number(s): 75.75.Cd, 75.60.Ch, 75.70.Ak

I. INTRODUCTION

For current-driven domain wall processing on nanosized magnetic stripes, a domain structure with highly symmetric domain patterns and with the magnetization direction perpendicular to the stripe axis would be favorable. This type of domain structure can be realized in ferromagnetic films with a uniaxial magnetic anisotropy axis perpendicular to the stripe axis.[1] Model systems for this situation in the literature are single-crystalline Co nanostripes with the magnetic easy axis perpendicular to the stripe axis[2–4] and Fe nanostripes grown epitaxially on GaAs.[5–7] However, the uniaxial anisotropy constant K_u of hexagonal Co ($K_u \approx 5 \times 10^5$ J/m^3) (Ref. 2) as well as for epitaxially grown Fe stripes ($K_u \approx 5 \times 10^4$ J/m^3) (Ref. 5) is relatively large, and since the critical current density for current-driven domain wall motion scales with the anisotropy energy,[8] domain wall motion by spin transfer torque would require very high current densities.

The ferromagnetic Heusler half metals such as Co_2MnGe have a cubic crystal structure and in the bulk exhibit a weak cubic magnetic anisotropy.[9] When grown as thin films they often develop a uniaxial magnetic anisotropy superimposed on an anisotropy with cubic symmetry. Examples in the literature are Co_2MnGe grown on GaAs(100) (Refs. 10–12) and Co_2MnGe grown on Al_2O_3 ($11\bar{2}0$).[13–15] Here we show that in nanosized stripes of Co_2MnGe grown on Al_2O_3, a growth-induced uniaxial anisotropy with a value of K_u approximately two orders of magnitude smaller than in single-crystalline Co is sufficient to induce the formation of similar highly symmetric perpendicular domain patterns.

In addition to the aforementioned magnetic anisotropy, ferromagnetic half metallic Heusler alloys, such as the title compound Co_2MnGe, have recently attracted much interest due to their large potential as spintronic materials.[16,17] One of the exceptional features of the half metallic Heusler compounds is the full spin polarization at the Fermi level, predicted theoretically for chemically perfectly ordered alloys.[18] Although, to the best of our knowledge, this full spin polarization has not been achieved yet in real devices, the very high tunnel magnetoresistance in magnetic tunneling junctions with Heusler electrodes demonstrate their technological potential.[19] Heusler alloys are also discussed as the material of choice for giant magnetoresistance (GMR)-based read heads in the next generation of hard disk drives,[20] and they possess a combination of properties,[21] making them ideally suited for applications using the spin torque transfer mechanism[22] such as the spin transfer torque oscillator,[23] or domain wall logic.[24] Recently it has been shown that the critical current density needed for current-driven magnetization reversal in a $Co_2MnAl_{0.5}Si_{0.5}$ Heusler nanocontact[25] was smaller than for similar Permalloy nanocontacts.[26]

II. PREPARATION AND EXPERIMENTAL

Thin films of Co_2MnGe were prepared by rf sputtering from a Heusler alloy target with a stoichiometric composition on ($11\bar{2}0$) Al_2O_3 substrates at a substrate temperature of 300 °C. Prior to the Co_2MnGe film growth, a 4-nm-thick V seed layer was deposited to induce a high-quality (110) textured growth of the Heusler layer (for details, see Ref. 27). A 5-nm-thick Au cap layer protects the film against oxidation. No further postgrowth treatment of the samples was applied. The crystallographic structure of the film was studied by an in-house x-ray diffractometer using Cu $K\alpha$ radiation. For in-plane rocking scans of selected samples we employed synchrotron radiation at the beam line W1.1 of the HaSyLab (DESY, Hamburg) on a six-circle diffractometer using a photon energy of 10 510 eV. The film thicknesses were checked by x-ray reflectivity measurements.

The x-ray out-of-plane Bragg scan of a 100-nm-thick Co_2MnGe film grown on Al_2O_3-($11\bar{2}0$) is depicted in Fig. 1. Besides the substrate Bragg reflections, only the Heusler Bragg reflections (220) and (440) appear, thus confirming the expected (110) out-of-plane texture of the film.

The in-plane rocking scan of the (022) Bragg reflection of the same sample is shown in Fig. 2. For pure epitaxial growth one would expect a twofold symmetry of the (022) reflection. The film, however, exhibits a $2 \times 6 = 12$-fold symmetry, i.e., six domains with twofold symmetry. The neighboring Bragg peaks enclose exactly 30° between each other. The *c* axis of the Al_2O_3 substrate points in the direction of one of the

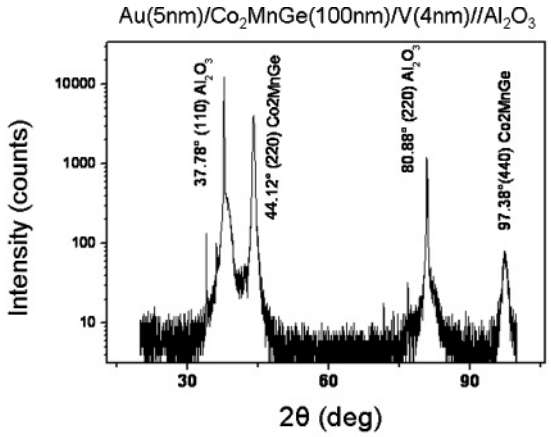

FIG. 1. Out-of-plane x-ray Bragg scan of a Co_2MnGe film on an Al_2O_3 *a* plane.

Bragg peaks and defines the in-plane rotation angle $\varphi = 0$ in the polar diagram. Thus in the film plane the Co_2MnGe layer exhibits a complex pseudoepitaxial crystallographic structure composed of six equivalent crystallographic domains with the [011] direction rotated by 30° relative to each other. A similar crystallographic structure has been reported before in Ref. 15.

Magnetic hysteresis loops of continuous Co_2MnGe films were recorded using a superconducting quantum interference device (SQUID)-based magnetometer (Quantum Design MPMS) and a magneto-optical Kerr effect (MOKE) setup.[28] During longitudinal MOKE measurements the hysteresis loops can be taken as a function of the in-plane azimuthal angle φ of the applied magnetic field with respect to the in-plane *c* direction of the *a* plane Al_2O_3 substrate. The results are discussed below.

For the analysis of magnetic domains in nanostructures, the Co_2MnGe films were shaped into nanosized rectangular stripes with different aspect ratios and different orientations by electron beam lithography and ion beam milling. MFM

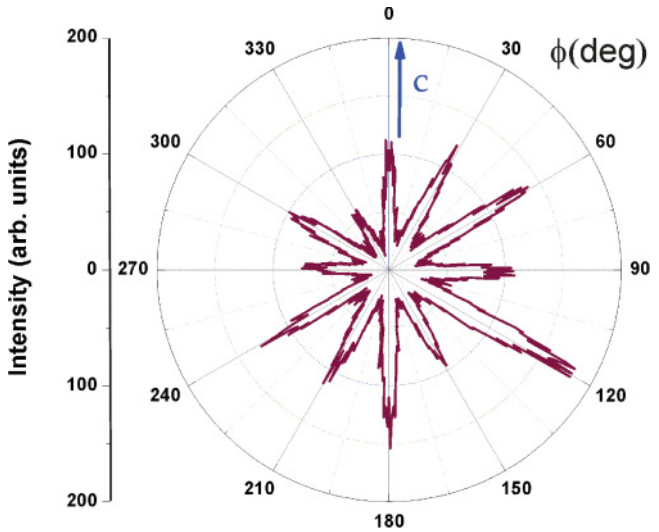

FIG. 2. (Color online) Polar plot of the in-plane rocking scan for the Co_2MnGe film from Fig. 1 recorded at the diffraction angle of the (022) Bragg reflection at $2\Theta = 33.64°$.

TABLE I. Parameters for Co_2MnGe films A–D discussed in this paper, including their film thickness *d*, the anisotropy constants K_u and K_4, and the ratio K_u/K_4. For experimental reasons (see main text) the determination of the anisotropy constants for sample D is rather uncertain.

Sample	*d* (nm)	K_u (10^3 J/m^3)	K_4 (10^3J/m^3)	K_u/K_4
A	100	6.1	0.31	19.6
B	100	4.5	0.77	5.8
C	60	3.7	1.18	3.1
D	60	(0.88)	(0.4)	(2.2)

images of the Co_2MnGe stripes were taken by a magnetic force microscope (NT-MDT), which allows the application of a magnetic field up to 8×10^4 A/m and a rotation of the sample plane with respect to the magnetic field direction (for details, see Ref. 29). In the following we will discuss in more detail four sample sets A–D, which are listed in Table I.

III. RESULTS AND DISCUSSION

A. Magnetic anisotropy

SQUID magnetometry measurements of the Co_2MnGe thin films grown on an Al_2O_3 *a* plane yielded a saturation magnetization corresponding to $3.4\mu_B$ per formula unit at 300 K and $3.7\mu_B$ at 4 K, which is ~80% of the theoretical saturation magnetization.[18] These values are attained after growth and without any further postgrowth processing. As shown in previous ferromagnetic resonance (FMR) investigations,[14,15] in our present Co_2MnGe films the magnetic anisotropy can be well described by a uniaxial anisotropy superimposed by a fourfold cubic symmetry anisotropy. The fourfold anisotropy adopts the symmetry of the $(11\bar{2}0)$ sapphire plane, with the symmetry axes given by the direction parallel and perpendicular to the *c* axis of the Al_2O_3 single crystal. The direction of the superimposed uniaxial anisotropy axis is usually close to the direction of the substrate *c* axis, although examples with other directions have also been found.[15] As evident from a comparison with the in-plane rocking scan shown in Fig. 2, the symmetry of the magnetic anisotropy axes is not directly related to the crystal symmetry of the Co_2MnGe thin film. It is rather determined by the symmetry of the substrate and probably originates from the lattice mismatch stress, induced during the pseudoepitaxial thin-film growth.[30]

In Fig. 3 we show hysteresis loops of four different Co_2MnGe films with nominal thicknesses of 100 nm (A, B) and 60 nm (C, D) measured by MOKE at room temperature for the field direction parallel to the *c* axis ($\varphi = 0°$) and perpendicular to the *c* axis ($\varphi = 90°$). For $\varphi = 0°$ the hysteresis loops exhibit easy-axis behavior with a square-shaped loop and a sharp reversal at the coercive force $\mu_0 H_c$ of the order of 2–4 mT. In the perpendicular direction ($\varphi = 90°$) sample A shows a typical hard-axis behavior with a linear, reversible $M(H)$ curve, as expected for a film with pure uniaxial magnetic anisotropy. Films B and C also exhibit in the perpendicular direction a typical hard-axis behavior, however, combined with a hysteretic jumplike approach to saturation at approximately $\mu_0 H = 7$ mT for sample B and $\mu_0 H = 3$ mT for sample C.

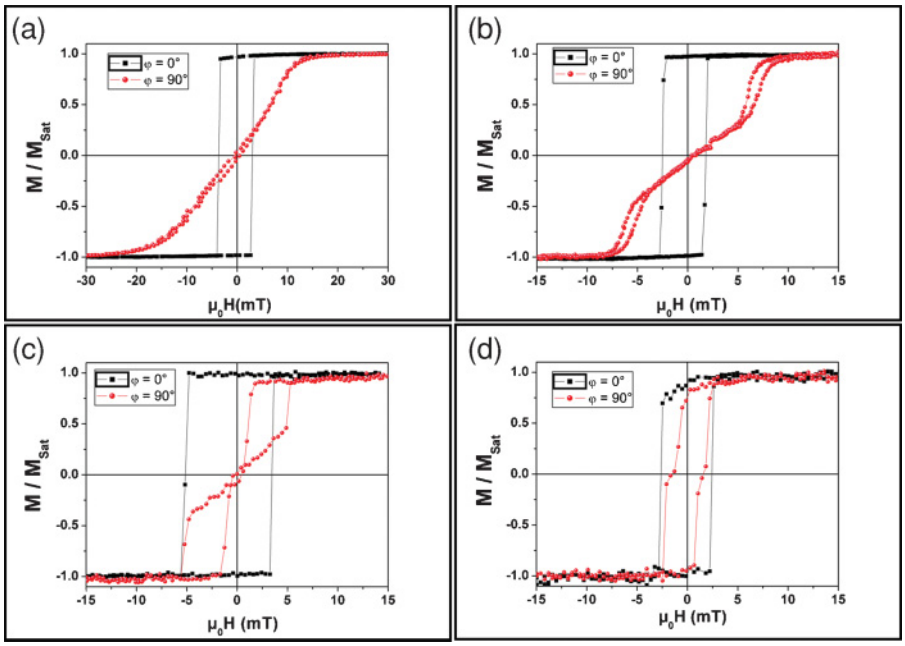

FIG. 3. (Color online) Magnetic hysteresis loops of Co_2MnGe films A–D for the direction parallel (squares) and perpendicular (filled circles) to the crystallographic c axis of the Al_2O_3 a-plane substrate. The labels A–D correspond to those in Table I.

This is indicative of a secondary easy axis perpendicular to the substrate c axis.[10] Sample D represents a special case with very similar hysteresis curves for field directions parallel and perpendicular to the c axis.

Qualitatively speaking, the change of the hard-axis loop shape from sample A to D indicates a decreasing strength of the uniaxial anisotropy as compared to the cubic anisotropy. The microscopic origin for the variation of the magnetic anisotropies in these films, which have all been prepared under identical conditions, is presently not clear. However, the large scattering of the anisotropy parameters (see Table I) is a characteristic feature of Heusler thin films.[30] The film thickness plays the dominant role,[15] and the substrate miscut and the specific substrate surface conditions also have an important influence.

Figure 4 shows a polar plot of the coercive field $H_c(\varphi)$ measured by MOKE for sample B as a function of the azimuthal angle φ. We notice a purely uniaxial anisotropy aligned with the substrate c axis ($\varphi = 0$) defining the symmetry axis. The coexisting fourfold symmetry cannot be resolved in this plot of $H_c(\varphi)$.

As explained above, the effective magnetic anisotropy energy for Co_2MnGe thin films grown on a-plane Al_2O_3 can be described by a superposition of a fourfold and a uniaxial anisotropy term.[11,14] The total magnetic energy density E_{mag} for the in-plane hard-axis hysteresis loops in Fig. 3 (magnetic field oriented perpendicular to the c axis of the substrate) can well be described by

$$E_{mag} = K_4 \cos^2(\Theta)\sin^2(\Theta) + K_u \cos^2(\Theta) - M_s H \cos(\Theta), \quad (1)$$

with the cubic anisotropy constant K_4, the uniaxial anisotropy constant K_u, the saturation magnetization M_s, and the angle Θ between the magnetization direction and the applied magnetic field. Setting the derivative $dE_{mag}/d\Theta = 0$, one can calculate the equilibrium angle Θ from Eq. (1) and simulate the magnetization curve $M(H)$ taking K_4 and K_u as the fitting parameters.

Alternatively, from the equilibrium condition $dE_{mag}/d\Theta = 0$ follows the magnetic saturation field H_s, defined as the field when the saturation magnetization is reached, yielding

$$H_s = 2(K_u - K_4)/M_s, \quad (2)$$

and the initial susceptibility

$$dM/dH = \tfrac{1}{2}M_s^2/(K_u + K_4). \quad (3)$$

Both experimental parameters can readily be obtained by inspection of Fig. 3, allowing a straightforward calculation of K_4 and K_u. The resulting anisotropy constants are summarized in Table I. We notice that the uniaxial anisotropy constant decreases and the cubic anisotropy constant increases continuously from sample A to sample C. The numerical values for the anisotropy constants provided in Table I are comparable to those derived previously from FMR measurements.[15] For sample D the derivation of the anisotropy constants K_4 and K_u

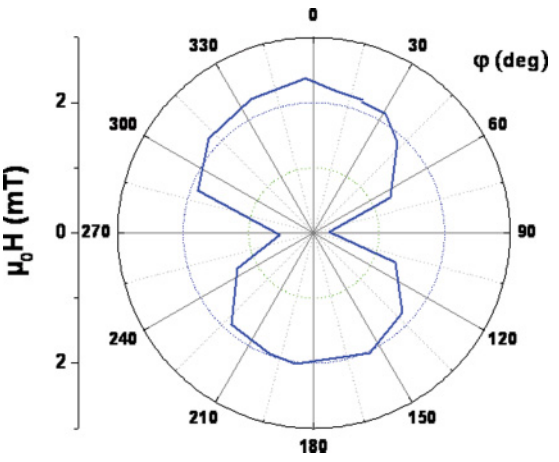

FIG. 4. (Color online) Coercive field $H_c(\varphi)$ for sample B as a function of the azimuthal angle φ, which denotes the angle of the magnetic field direction with the c axis of the substrate. The data points are connected by straight lines as a guide to the eye.

is rather uncertain experimentally, because for the hard-axis direction the coercive field and the saturation field are of the same order of magnitude. However, for this sample the anisotropy constants are exceptionally small.

B. Magnetic domains of Co_2MnGe nanostripes

From the Co_2MnGe films A–D discussed before we prepared by means of *e*-beam lithography stripes with different widths w varying between 0.3 and 5.5 μm and lengths L varying between 2 and 100 μm. Referring to the discussion in the Introduction, the first important question to be answered is whether the uniaxial anisotropy is sufficiently strong to induce a domain pattern with the magnetization direction perpendicular to the stripe axis.

In Fig. 5 we show the MFM images of stripes with the dimensions $w = 400$ nm and $L = 5.5$ μm, prepared from films B and C. Before recording the images, the stripes were magnetically saturated along the magnetic easy axis defined for the homogeneous film and indicated by white arrows labeled K_u in Fig. 5. In the case of sample C shown in the upper part of Fig. 5, we observe typical MFM images of single-domain magnetic dipoles oriented along the long axis of the stripe. This longitudinal magnetic dipole state is observed for both stripe orientations, i.e., parallel as well as perpendicular to the direction of K_u. Obviously, for these stripes the uniaxial anisotropy is not strong enough to stabilize the magnetization direction perpendicular to the stripe axis. In the bottom part of Fig. 5 we show MFM images for stripes prepared from film B that has a larger K_u (see Table I). Here we observe again a single-domain magnetic dipole state for the stripes oriented parallel to the easy axis. However, for the perpendicular orientation (bottom image in Fig. 5) the MFM images reveal a highly symmetric multidomain pattern. The magnetization direction alternates perpendicular to the stripe axis, separated by 180° domain walls. The domain size δ parallel to the stripe axis is highly regular and has an average value of $\delta = 420 \pm 40$ nm. Thus for this sample the uniaxial anisotropy is strong enough to stabilize a perpendicular domain structure with the magnetization directions opposing the demagnetizing fields emanating from the edges of the stripe.

At this instance some numerical estimates concerning the stability of the domain structures for the nanostripes in Fig. 5 seem worthwhile. With the stripe geometry of sample B (width $w = 400$ nm, thickness $d = 100$ nm, length $L = 5500$ nm) and assuming a single-domain state with the magnetization direction perpendicular to the stripe axis, we estimate a demagnetizing factor $N_D = 0.22$.[31] With the saturation magnetization $M_s = 6.3 \times 10^5$ A/m of our Co_2MnGe film this gives a demagnetizing field $H_D = 1.4 \times 10^5$ A/m and a demagnetizing energy density $E_D = \frac{1}{2}\mu_0 H_D M_s = 5.6 \times 10^4$ J/m^3. This is approximately an order of magnitude larger than the uniaxial anisotropy energy density K_u (see Table I), thus a perpendicular single-domain state would be highly unstable.

In the perpendicular multidomain state with the alternating magnetization directions of neighboring domains, the demagnetizing field and the demagnetizing energy is strongly reduced, however, at the expense of an additional magnetic domain wall energy E_{DW}. Assuming straight domain walls the

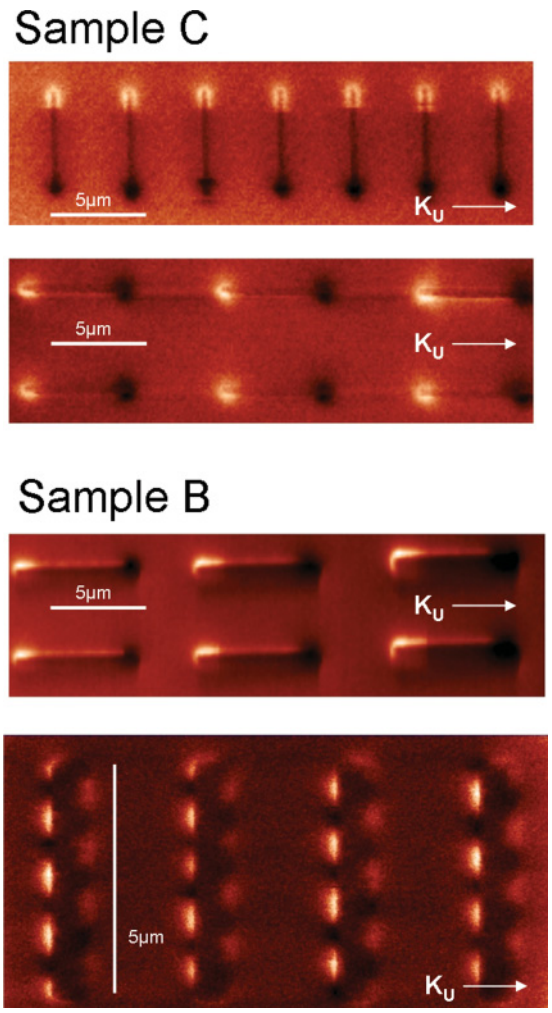

FIG. 5. (Color online) MFM images of Co_2MnGe stripes with $L = 5.5$ μm and $w = 400$ nm prepared from samples B and C (see Table I). The images were taken in the remanent state after magnetic saturation along the magnetic easy axis, which is oriented as indicated by the white arrow labeled K_u.

domain wall energy density E_{DW} can be estimated by

$$E_W = 4\sqrt{AK_u}\frac{1}{\delta}, \tag{4}$$

with the exchange energy constant A, the uniaxial anisotropy constant K_u, and the domain size along the stripe axis δ.[1] Using this formula we neglect the small cubic anisotropy. With the exchange energy constant $A = 1.1 \times 10^{-11}$ J/m for the Co_2MnGe phase taken from the literature[30] and the domain size $\delta = 420$ nm deduced from the domain image in Fig. 5, we calculate $E_{DW} = 1750$ J/m^3. This is definitely smaller than the uniaxial anisotropy energy, as prerequisite for the stability of the perpendicular multidomain state in competition with the single-domain state with the magnetization direction along the stripe axis.

However, the situation with the Co_2MnGe stripes is more complex, since the assumption of straight domain walls is unrealistic for our Co_2MnGe stripes. The domain structure for stripes with a dominating uniaxial anisotropy depends on the ratio of the anisotropy energy and the demagnetizing energy $Q = K_u/(\frac{1}{2}\mu_0 H_D M_s)$.[32] For $Q \ll 1$ complete flux closure is

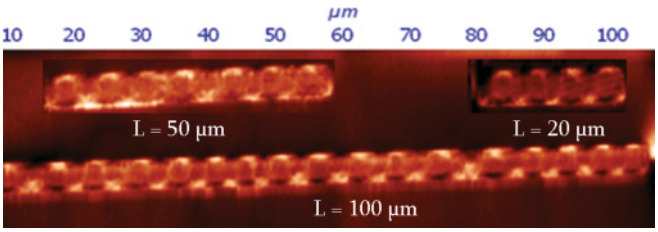

FIG. 6. (Color online) MFM images in the remanent state of stripes with $w = 5.5$ μm and different lengths L. The uniaxial easy axis is oriented perpendicular to the stripe axis.

expected, and for $Q > 1$ one expects straight stripe domains separated by 180° domain walls. Our system with $Q \approx 0.15$ comes close to the first limit, and thus the formation of flux closure domains at the edges of the perpendicular domains is expected. These closure domains are not directly visible in the MFM images, but are clearly seen in the object-oriented micromagnetic framework (OOMMF) simulations of the domain patterns (see Fig. 7 below). The role of the closure domains is to reduce the demagnetizing energy further, however, at the expense of an increasing wall energy density E_{DW} and an additional anisotropy energy density E_{an}. From the OOMMF simulations (see below) we conclude that the closure domains cover ~30% of each domain area, resulting in a contribution $E_{an} = 1350$ J/m^3. The total wall energy density, including the 90° walls of the closure domains, can be estimated to give $E_{DW} = 1900$ J/m^3, thus the total magnetic energy density (neglecting any residual demagnetizing energy) amounts to $E_{mag} = 3250$ J/m^3. One recognizes that this energy density is only slightly smaller than the anisotropy energy density $K_u = 4500$ J/m^3. This is consistent with the observation that for this particular sample the multidomain state really exists. However, it also indicates that the parameters for sample B already come very close to the stability limit for the perpendicular domain structure. In sample C with slightly different parameters in favor of the longitudinal single-domain state (smaller K_u, larger K_4) the situation is reversed and the perpendicular multidomain state is not stable anymore. The stability limit also depends on the geometrical parameters of the stripes, and holds only for stripes with similar aspect and thickness and width ratios.

C. Dependence of domain size on stripe geometry

In the following we study domain patterns for stripes with different geometries, but all prepared from the same film B from Table I. In Fig. 6 we show domain patterns in magnetic remanence for stripes with different aspect ratios L/w, keeping the width of the stripes constant at $w = 5.5$ μm and varying the length between 25 and 100 μm. We find that the average perpendicular domain size $\delta = 2.8 \pm 0.2$ μm is independent of the stripe length. This generally holds for aspect ratios $L/w > 5$. Thus apart from the closure domains at the two ends of the stripe, for $L/w > 5$, the vertical domain size δ is independent of the length and is identical to the one expected for an infinitely long stripe.

In Fig. 7 we show the perpendicular domain pattern for stripes with identical length $L = 5.5$ μm and different widths in the pristine state of the sample, i.e., before exposing the sample to any external magnetic field. We notice that the perpendicular domain size δ parallel to the stripe axis increases continuously with increasing stripe width w. After magnetic saturation along the stripe axis we obtain the same domain pattern, suggesting that the domain patterns in Fig. 7 represent the equilibrium domain state. This is corroborated by analyzing the domain patterns during the remagnetization process, as discussed further below. We also notice from Fig. 7 that the perpendicular domain size δ increases continuously with increasing stripe width w. The numerical values of δ and w are comparable, thus the domains have a quadratic shape, approximately.

In Fig. 7 we also present OOMMF simulations of the domain pattern of the stripes with a set of parameters derived from our experiments (saturation magnetization $M_s = 6.3 \times 10^5$ A/m, and anisotropy constants K_u and K_4 taken from Table I) and with the exchange stiffness constant $A = 1.1 \times 10^{-11}$ J/m taken from Ref. 30. The simulations started with a randomly demagnetized state and used a cell size of 10 nm. The simulated patterns are in good agreement with the experimental ones and clearly demonstrate the formation of closure domains with a magnetization direction parallel to the edges of the stripes, which cannot be resolved in the MFM images.

The classical result for the ground-state magnetic domain structure in a system with uniaxial magnetic anisotropy perpendicular to the stripe axis and complete flux closure is a regular domain pattern with the domain width δ along the axis of the stripe of width w given by[1]

$$\delta = 2\sqrt{2w\sqrt{A/K_u}}. \quad (5)$$

The experimentally determined domain width as a function of the stripe width is plotted in Fig. 8 together with the domain width deduced from the micromagnetic simulations, and both sets of data are in reasonable agreement. The theoretical curve using Eq. (5) with the parameters for our samples given above approximates the experimental domain size rather well for the lowest stripe widths, but for larger stripe widths there is an increasing deviation. The deviation probably originates from the coexisting cubic anisotropy K_4, which is neglected when using Eq. (5), and the fact that the flux closure in our stripes is not complete. This is evident from the OOMMF simulations as well as from the mere fact that the MFM images reveal

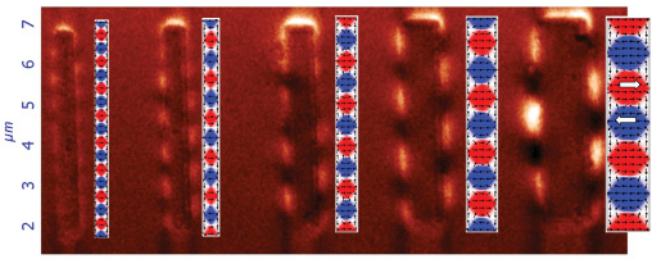

FIG. 7. (Color online) MFM images and OOMMF simulations of Co_2MnGe stripes of width $w = 300$, 400, 550, 750, and 1100 nm (from the left-hand side to the right-hand side). The uniaxial anisotropy axis is directed perpendicular to the long axis of the stripes. In the OOMMF simulations the direction of the magnetization is indicated by arrows.

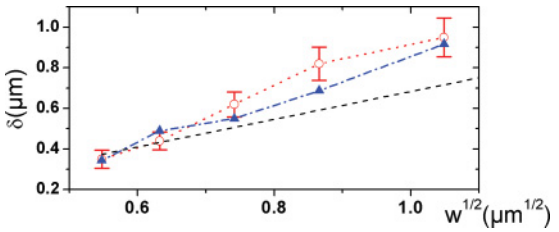

FIG. 8. (Color online) Open circles: Domain width δ in the direction of the stripe axis for Co_2MnGe stripes as function of the square root of the stripe width w. Triangles: Domain width deduced from the OOMMF simulations. Dashed line: Theoretical curve using Eq. (5).

the existence of magnetic stray fields from the perpendicular domains.

D. Magnetization reversal of nanosized stripes

In Fig. 9 we show hysteresis loops measured on stripes prepared from film A (Table I) with the dimensions $L = 5.5\ \mu$m and $w = 750$ nm. The direction of the uniaxial easy axis is oriented perpendicular to the stripes. First, hysteresis loops were measured by SQUID magnetometry and MOKE for the field directions perpendicular and parallel to the stripe axis (upper and lower panel in Fig. 9). Then MFM images were recorded at different positions along the hysteresis loops, starting from magnetic saturation at positive fields with the magnetic field in the MFM also applied perpendicular (upper panel) and parallel (lower panel) to the stripe axis.

For the field direction perpendicular to the stripe axis (the upper part of Fig. 9 in magnetic saturation) we observe a single domain state with the typical stray field of a dipole with the axis perpendicular to the stripe axis [position label (a) on the hysteresis loop]. Upon lowering the field slightly [label (b)], perpendicular domains with a highly regular pattern appear, aside from closure domains at the two ends of the stripe. The number of the domains does not change when lowering the field further [(c) to (d)], only the width of the domains changes. The domain size for domains with their magnetization direction parallel to the applied field shrinks, whereas the domain size for domains with antiparallel magnetization direction expands. This continues until eventually, at remanence, both domain sizes are identical. The remagnetization processes on the hysteresis loops are identical for all four branches of the hysteresis loops, i.e., the sequence of domain patterns (a)–(e) is just repeated along all four branches. From this we may infer that the magnetization reversal for the field direction perpendicular to the stripe axis is controlled by a nucleation process of a highly symmetric domain pattern just below the saturation field and domain wall movements in the direction perpendicular to the field for the remaining part of the hysteresis loop. The nucleation field of domain walls in a perfectly homogeneous ferromagnet is identical to the anisotropy field, which in our case is $H_{an} = 2(K_u + K_4)/(\mu_0 M_s) = 1.5 \times 10^4$ A/m. The demagnetizing field in the perpendicular direction of the stripe amounts to $H_D = 7.9 \times 10^4$ A/m and is thus a factor of $\sim$5 larger than the nucleation field. In this situation domain walls can nucleate easily at any position along the stripe and

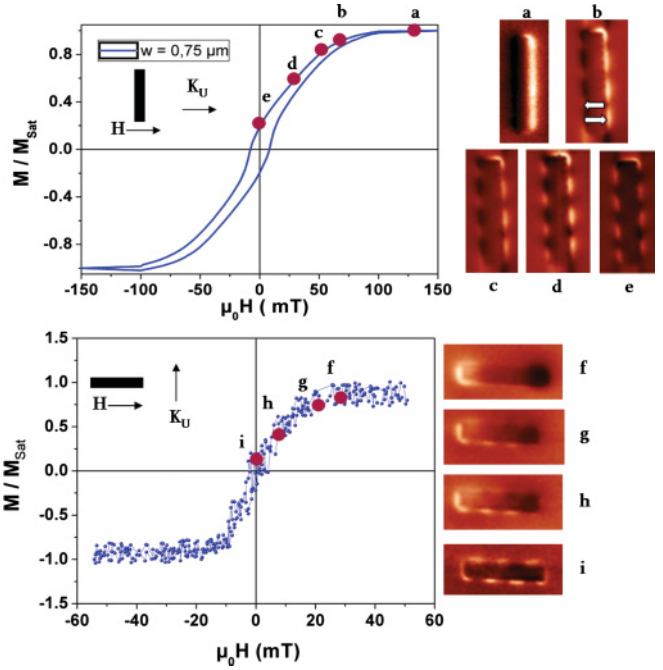

FIG. 9. (Color online) Hysteresis loops and MFM images taken during magnetization reversal for stripes with the dimensions $w = 750$ nm and $L = 5.5\ \mu$m. The uniaxial anisotropy direction is always directed perpendicular to the stripe axis. The magnetic field is applied perpendicular (upper figure) and parallel (lower figure) to the stripe axis. The labels (a)–(i) denote the position on the hysteresis loop and the corresponding domain image. One should note that the upper hysteresis loop has been measured by SQUID magnetometry, and the lower by MOKE.

the equilibrium distribution of the domain walls is readily established.

The magnetization reversal for the field oriented parallel to the stripe axis is shown in the lower part of Fig. 9. Starting from the single-domain dipole state with the dipole axis parallel to the stripe in magnetic saturation [label (f)], highly symmetric domains with stray fields perpendicular to the main magnetization direction nucleate when lowering the field slightly [label (g)]. The strong stray fields at both ends of the stripe, however, still exist, which is indicative for a rotation of the magnetization direction inside the domains toward the long axis of the stripes. Eventually, in magnetic remanence, the domain pattern is virtually indistinguishable from the one we observed for the perpendicular field orientation. These domain patterns are again identical for all branches of the hysteresis loop. We may conclude that the remagnetization process for the field direction parallel to the stripe axis is also initiated by the nucleation of a highly symmetric perpendicular domain pattern just below the saturation field, and then is continued by coherent rotation of the magnetization direction inside the domains for the remaining part of the magnetization curve. For the orientation of the magnetic field parallel to the stripe axis with the present stripe geometry there is still a sizable demagnetizing field of $H_D = 1.2 \times 10^4$ A/m, which is still of the same order of magnitude as the field for homogeneous domain wall nucleation. This explains the model

character of remagnetization behavior which we also observe for the longitudinal magnetization direction.

There are two remarkable features in these observations, which we wish to point out: First, the domain structure in remanence does not depend on the magnetic history of the stripe and is identical after saturation parallel and perpendicular to the stripe axis, very unlike the situation, e.g., in Co nanostripes.[2] This suggests that the remanent domain state which we observe is indeed the thermodynamic magnetic ground state. The basic reason for this is the small nucleation energy of domain walls in our stripes, which enables homogeneous domain wall nucleation. Second, the highly regular domain patterns and the similarity of the domain state in different stripes indicates that the pinning forces for domain walls in these stripes is very weak so that each domain wall can readily reach its equilibrium position. Since the pinning forces usually scale with the domain wall energy, this is also essentially due to the rather weak uniaxial anisotropy in the Heusler alloy Co_2MnGe.

IV. SUMMARY AND CONCLUSIONS

In summary, we have grown by rf-sputtering methods thin films of the Heusler compound Co_2MnGe on *a*-plane Al_2O_3 substrates. The Heusler films have a pseudoepitaxial structure with the [110] axis perpendicular to the film plane and six crystallographic {011}-oriented domains in the film plane. The magnetic anisotropy is characterized by a fourfold anisotropy superimposed by a twofold anisotropy. The symmetry of the magnetic anisotropy is defined by the symmetry of the substrate plane and is not directly related to crystal symmetry of the Co_2MnGe film. The magnitude of the twofold and fourfold anisotropy constants depends on the growth conditions and can vary appreciably. The origin of both anisotropy contributions is still a question of debate in the literature,[13,30] however, it can be stated that good pseudomorphic growth is beneficial for a uniaxial anisotropy in the Co_2MnGe films. Furthermore, the films should not be too thin—100 nm appears to be an optimal thickness. This may indicate that K_u is only indirectly affected by the interface.

In nanostructured stripes oriented with the long axis perpendicular to the uniaxial easy axis, we observe the formation of highly symmetric domain patterns. These patterns have their magnetization direction perpendicular to the stripe axis. We have shown that a uniaxial anisotropy constant of 4.500 J/m^3 is sufficient to stabilize this particular domain pattern in magnetic remanence, which is approximately two orders of magnitude smaller than in Co nanostripes.[2] This value comes very close to the critical lower limit of K_u for this particular domain state, since for a slightly smaller K_u value we observe that a magnetic dipole state parallel to the stripe axis becomes the stable ground state in remanence, irrespective of the orientation of the stripe axis. Furthermore, we have established the dependence of the domain width δ as a function of stripe width w in the ground state and found that this dependence is reasonably well described by the classical Kittel formula only for small stripe width.[1]

In conclusion, the ferromagnetic Heusler half metals such as the title compound Co_2MnGe combine a high degree of spin polarization, weak uniaxial anisotropy in thin films, and weak pinning forces for domain walls in nanostructures, making them promising candidates for applications related to the control and manipulation of magnetic domain walls by current-driven spin transfer torque, such as the magnetic storage device proposed in Ref. 33.

ACKNOWLEDGMENTS

The authors would like to thank Sabine Erdt-Böhm and Peter Stauche for technical help and the SFB 491 as well as the state of NRW for financial support of the *e*-beam lithography and MFM facilities. One of us (K.G.) also wants to thank the DAAD for support.

[1] C. Kittel, Phys. Rev. **70**, 965 (1946).
[2] W. Bruckner, J. Thomas, R. Hertel, R. Schäfer, and C. M. Schneider, J. Magn. Magn. Mater. **283**, 82 (2004).
[3] I. L. Prejbeanu, L. D. Buda, U. Ebels, M. Viret, C. Fermon, and K. Ounadjela, IEEE Trans. Magn. **37**, 2108 (2001).
[4] S. Cherifi, R. Hertel, A. Locatelli, Y. Watanabe, G. Potdevin, A. Ballestrazzi, M. Balboni, and S. Heun, Appl. Phys. Lett. **91**, 092502 (2007).
[5] U. Rüdiger, J. Yu, S. A. D. Kent, and S. P. Parkin, Appl. Phys. Lett. **73**, 1298 (1998).
[6] R. Pulwey, M. Zölfl, G. Bayreuther, and D. Weiss, J. Appl. Phys. **91**, 7995 (2002).
[7] C. Hassel, S. Stienen, F. M. Römer, R. Meckenstock, G. Dumpich, and J. Lindner, Appl. Phys. Lett. **95**, 032504 (2009).
[8] G. Tatara and H. Kohno, Phys. Rev. Lett. **92**, 086601 (2004).
[9] B. Michelutti, R. P. de la Bathie, and E. du Tremolet de Lacheisserie, Solid State Commun. **25**, 163 (1978).
[10] F. Y. Yang, C. H. Shang, C. L. Chien, T. Ambrose, J. J. Krebs, G. A. Prinz, V. I. Nikitenko, V. S. Gornakov, A. J. Shapiro, and R. D. Shull, Phys. Rev. B **65**, 174410 (2002).
[11] T. Ambrose, J. J. Krebs, and G. A. Prinz, Appl. Phys. Lett. **76**, 3280 (2000).
[12] T. Ambrose, J. J. Krebs, and G. A. Prinz, J. Appl. Phys. **87**, 5463 (2000).
[13] M. Belmeguenai, F. Zighem, T. Chauveau, Y. Roussigné, S-M. Chérif, P. Moch, K. Westerholt, and Ph. Monod, J. Appl. Phys. **108**, 063926 (2010).
[14] M. Belmeguenai, F. Zighem, G. Woltersdorf, Y. Roussigné, S.-M. Chérif, K. Westerholt, and G. Bayreuther, J. Magn. Magn. Mater. **321**, 750 (2009).
[15] M. Belmeguenai, F. Zighem, Y. Roussigné, S.-M. Chérif, P. Moch, K. Westerholt, G. Woltersdorf, and G. Bayreuther, Phys. Rev. B **79**, 024419 (2009).
[16] I. Zutic, J. Tabian, and S. Das Sarma, Rev. Mod. Phys. **78**, 323 (2004).
[17] H. Zabel, Superlattices Microstruct. **46**, 451 (2009).

[18] *Half-Metallic Alloys, Fundamentals and Applications*, edited by I. Galanakis and P. H. Dederichs (Springer, Berlin, 2005).
[19] S. Tsunegi, Y. Sakuraba, M. Oogane, K. Takanashi, and Y. Ando, Appl. Phys. Lett. **93**, 112506 (2008).
[20] T. Furubayashi, K. Kodama, H. Sukegawa, Y. K. Takahashi, K. Inomata, and K. Hono, Appl. Phys. Lett. **93**, 122507 (2008).
[21] T. Kubota, S. Tsunegi, M. Oogane, S. Mizukami, T. Miyazaki, H. Naganuma, and Y. Ando, Appl. Phys. Lett. **94**, 122504 (2009).
[22] L. Berger, Phys. Rev. B **54**, 9353 (1996); J. C. Slonczewski, J. Magn. Magn. Mater. **159**, L1 (1996).
[23] A. Slavin and V. Tiberkevich, IEEE Trans. Magn. **45**, 1875 (2009).
[24] R. P. Cowburn and M. E. Welland, Science **287**, 1466 (2000).
[25] H. Sukegawa, S. Kasai, T. Furubayashi, S. Mitani, and K. Inomata, Appl. Phys. Lett. **96**, 042508 (2010).
[26] P. M. Braganca, I. N. Krivorotov, O. Ozatay, A. Garcia, N. C. Emley, R. C. Sankey, and R. A. Buhrman, Appl. Phys. Lett. **87**, 112507 (2005).
[27] U. Geiersbach, A. Bergmann, and K. Westerholt, Thin Solid Films **425**, 225 (2003).
[28] A. Westfalen, M.-S. Lee, A. Remhof, and H. Zabel, Rev. Sci. Instrum. **78**, 121301 (2007).
[29] A. Schumann, B. Sothmann, P. Szary, and H. Zabel, Appl. Phys. Lett. **97**, 022509 (2010).
[30] S. Trudel, O. Gaier, J. Hamrle, and B. Hillebrands, J. Phys. D **43**, 193001 (2010).
[31] A. Aharoni, J. Appl. Phys. **83**, 3432 (1998).
[32] A. Hubert and R. Schaefer, *Magnetic Domains* (Springer, Berlin, 1998).
[33] S. S. P. Parkin, Science **320**, 190 (2008).